MODELING INTERFACIAL TENSION EFFECTS IN NUMERICAL SIMULATIONS

Karime Louise Zenedin Glitz, karime@sinmec.ufsc.br
António Fábio Carvalho da Silva, afabio@sinmec.ufsc.br
Clovis Raimundo Maliska, maliska@sinmec.ufsc.br
SINMEC – Computational Fluid Dynamics Lab. Mechanical Engineering Department, UFSC. CEP: 88040-970, Florianópolis-SC, Brazil. Phone: +55 48 3721 9562

Abstract. *Interfacial tension plays an important role in a large variety of problems, such as ink-jet printing, emulsification and break-up of liquid jets. Flows involving interfacial tension effects can be simulated numerically by the inclusion of these effects in the equations for conservation of momentum through a model. When a volume method – like the Volume of Fluid (VOF) method – is employed to track the position of the interface, the treatment of the interfacial tension effects becomes a complex task, as they must be considered at such a narrow region as is the interface. In order to deal with this difficulty the Continuum Surface Force model (CSF) was developed. In this model the force due to interfacial tension is included in the Navier-Stokes equations as a body force, which acts in a limited region around the interface. One of the variables considered in the evaluation of this force is the curvature of the interface. The major aim of this paper is to present some models of assessment of this variable and to compare the results obtained by each one of them. In this work the following curvature-models were implemented: Height Function method (HF), Convolution technique, Height Function filtered by a convolution kernel (HF-fc), and an enhanced Height Function method (HF2). This last model is proposed by the authors as it was observed that the spurious currents generated by the HF method were associated to the local anisotropy of the curvature field and to errors in its estimation. In order to compare these models two test cases were simulated: the static drop in equilibrium and the rising bubble in a resting fluid. The results were compared to those published in the literature. In the static drop case when the L_2 error norm of the velocity was analyzed, it was observed first-order convergence for the convolution technique, while it was verified second-order convergence for the three other models. However, there is an increasing tendency in this error for the HF method when fine meshes are used. This is also the overall behavior for the L_2 error norm for the curvature. The results for the rising bubble show that good agreement to those published in literature is achieved by the HF and HF2 methods, while the effects of spurious currents are more pronounced in the results obtained by the other two models.*

Keywords: interfacial tension, curvature models, VOF, CSF

1. INTRODUCTION

Interfacial tension plays an important role in a large variety of problems, such as ink-jet printing, emulsification and break-up of liquid jets. This property of the fluids represents the action of the molecules in the interface between the fluids: while the molecules in bulk fluid are subjected to equal attractive forces from all the sides, those molecules in the interface are subjected to a weaker force of the neighbour fluid molecules – considering a lighter neighbour fluid. Thus the resultant force acting in these molecules tends to "pull" them to the bulk fluid. As a result the surface interfacial area is decreased. This behaviour explains why a resting drop of water has a spherical shape.

The force due to interfacial tension acts only at the interface between the fluids, which is a narrow region with only some angstroms thickness. This characteristic makes the computational modeling of interfacial tension effects a hard task: in two-dimensional flows these effects must be considered only at a line while in three-dimensional flows, they are considered at a surface.

To overcome this difficulty Brackbill and coworkers (1992) developed the Continuum Surface Force (CSF) model. In this model the interfacial tension effects are included in the Navier-Stokes equations through a body force, which acts in a limited region around the interface.

One of the variables considered in the evaluation of this force is the curvature of the interface. Then the major aim of this paper is to present some models of assessment of the curvature in the calculation of the force and to compare the results obtained by each one of them. In this work the following curvature-models were implemented: Height Function method (HF), Convolution technique, Height Function filtered by a convolution kernel, and an enhanced Height Function method (HF2). This last model is proposed by the authors as it was observed that the spurious currents generated by the HF method were associated to the local anisotropy in the curvature field and to the errors in its estimation. In order to compare these models two test cases were simulated: the static drop in equilibrium and the rising bubble in a resting fluid. The results were compared to those published in the literature.

2. NUMERICAL MODEL

The numerical simulations carried out considered two-dimensional transient flow of two fluids with different physical properties. Both the fluids are considered incompressible.

As the interface between the fluids is well-defined in both the test-cases, the Navier-Stokes (NS) equations are solved for each phase, and the physical properties of the mixture (named the viscosity and the density of the fluid) are considered in the NS equations when assessing the flow in the interface region. Thus the governing equations of this flow are

$$\frac{\partial f_k}{\partial t} + \nabla \cdot \left(f_k \mathbf{u} \right) = 0 \tag{1}$$

which is the equation of continuity applied to both fluids,

$$\frac{\partial \rho}{\partial t} + \nabla \cdot \left(\rho \mathbf{u} \right) = 0 \tag{2}$$

which is the equation of continuity for the mixture, and

$$\frac{\partial \left(\rho \mathbf{u} \right)}{\partial t} + \nabla \cdot \left(\rho \mathbf{u}\mathbf{u} \right) = -\nabla p + \nabla \cdot \left\{ \mu \left[\nabla \mathbf{u} + \left(\nabla \mathbf{u} \right)^T \right] \right\} + \rho \mathbf{b} + \mathbf{F}_{sv} \tag{3}$$

which is the momentum equation.

In these equations f_k denotes the volume fraction of the fluid k, $\mathbf{u}$ denotes the velocity vector $\mathbf{u} = (u,v)$, t represents time and p denotes pressure. The last two terms in the right-hand side of Eq. (3) correspond to the body forces and to the force due to the interfacial tension, respectively. The density and the dynamic viscosity of the mixture are denoted by ρ and μ, respectively. These physical properties are estimated by averaging each fluid property weighted by its volume fraction. Therefore for a two-phase flow:

$$\rho = f_1 \rho_1 + f_2 \rho_2 \tag{4}$$

$$\mu = f_1 \mu_1 + f_2 \mu_2 \tag{5}$$

where the subindexes denote the fluid.

In order to numerically solve the flow, i.e., to determine the fields of u, v, p, ρ and μ, the Finite Volume method (FVM) was applied to the governing equations, by dividing the domain into discrete volumes and integrating these equations over these volumes and over time intervals. The PRessure Implicit Momentum Explicit (PRIME) method was used to treat the pressure-velocity coupling problem (Maliska, 2004).

2.1. Interface tracking

Since the main objective of this work is to evaluate different curvature-models, the interface must be well-defined and its position must be determined accurately. Thus the Volume-of-fluid (VOF) method is applied in the simulations (Hirt and Nichols, 1981). In this method Eq. (1) is solved by determining the volume fraction field. As this task involves the assessment of the fluxes of f advected through the boundaries of the control volume, the Piecewise-Linear Interface Calculation (PLIC) technique, which approximates the interface by linear oriented-segments, was employed (Malik and Bussmann, 2004; Kothe *et al.*, 1996). The association between the VOF method to this reconstruction technique should provide a well-defined interface, whose position is also well-determined.

2.2. Interfacial tension effects

When the VOF method is employed to track the position of the interface, the treatment of the interfacial tension effects becomes a complex task, as these effects must be considered only at such a narrow region as is the interface between the fluids.

In order to deal with this problem Brackbill and coworkers (1992) developed the Continuum Surface Force (CSF) model. In this model the force due to interfacial tension is included in the Navier-Stokes equations as a body force ($\mathbf{F}_{sv}$), which acts in a limited region around the interface. This force is the product among the interfacial tension coefficient (σ), the curvature of the interface (κ), the unit vector normal to the interface ($\hat{\mathbf{n}}$) and the Dirac Delta function (δ), given by:

$$\mathbf{F}_{sv} = \sigma \kappa \hat{\mathbf{n}} \delta \tag{6}$$

As the vector normal to the interface is defined as the gradient of the volume fraction, it was evaluated by employing a finite difference approach in a 3x3-volumes stencil. The Dirac delta function was taken to be equal to $\left| \nabla f_l \right|$, constraining the action of this force to the interfacial volumes.

2.3. Curvature models

The curvature of the interface is defined as

$$\kappa = -\nabla \cdot \hat{\mathbf{n}} \tag{7}$$

In the literature there are plenty works about the estimation of this variable, where various different models are proposed. Four of these models were employed in this work and their results were compared among each other and to those of the literature. These models are: Height Function (HF) method, Convolution technique, Height Function filtered with a convolution kernel (HF-fc), and an enhanced Height Function method (HF2).

2.3.1. Height function method

In the HF method the interface is approximated by a height function (Sussman and Ohta, 2006; Malik, Fan and Bussmann, 2007; López *et al.*, 2009). And, since the curvature is defined by Eq. (7) it results that

$$\kappa_{i,j} = -\frac{H_{xx}}{\left(1 + H_x^2\right)^{3/2}} \tag{8}$$

where H is the discrete height function evaluate at the volume (i,j), and the subindexes denote differentiation.

The values of H are determined by taking a stencil according the direction at which the volume fraction most varies (dominant direction of f): if the dominant direction is the x-direction, then a 7x3-volumes stencil should be taken, otherwise a 3x7-volumes stencil should be employed. The differentiation in Eq. (8) depends on this dominant direction: if this direction is the x-direction, the derivatives relative to y should be calculated, and vice-versa.

Figure 1 shows an example of such a stencil applied to the estimation of the curvature of the central volume.
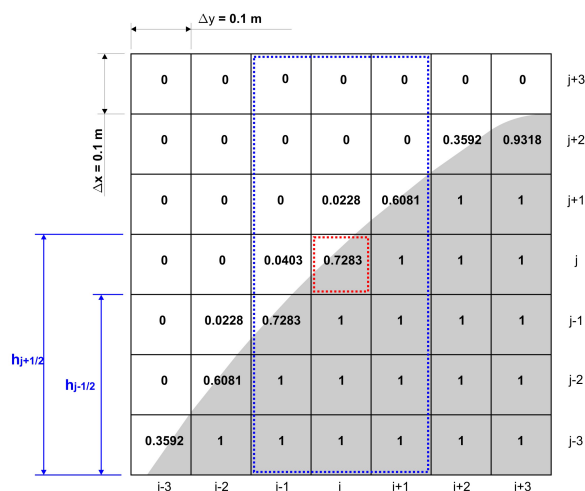

Figure 1. Example of the volume fraction field (gray = fluid 1 and white = fluid 2).

As in this figure the gradient of the volume fraction is higher in the *y*-direction, a 3x7 volumes stencil is chosen and the Height function is expressed as:

$$H_i = \sum_{k=j-3}^{j+3} f_{i,k} \cdot \Delta y_{i,k} \tag{9}$$

where Δy denotes the increment in space in the y-direction.

The derivatives in Eq. (8) are estimated by employing a finite difference approximation. Thus for the volume fraction field illustrated in Fig. 1 the curvature obtained numerically for the volume (i,j) is equal to 0.5004 m^{-1}, while its exact value is 0.5 m^{-1}.

An important detail about this method is that H_i must satisfy the following criterium:

$$h_{j-1/2} < H_i < h_{j+1/2} \tag{10}$$

where the limits $h_{j-1/2}$ and $h_{j+1/2}$ are shown in Fig. 1.

If this criterium is not satisfied $\kappa_{i,j}$ must assume the same value of the curvature of the nearest volume at which the condition (10) is satisfied.

As will be shown in section 4 this constrain implies a local anisotropy in the curvature field. A suitable treatment of this anisotropy leads to the development of the HF2 method, as will be further discussed.

2.3.2. Convolution technique

The main objective of this technique is to smooth the volume fraction field in a region around the interface, resulting in a smoothed volume fraction field ($\tilde{f}$), and therefore in a diffuse interface only for curvature calculation purposes (Williams *et al.*, 1998).

In this model a convolution operation between the volume fraction field and a kernel $\mathbf{K}(\mathbf{x})$ is applied, resulting in the $\tilde{f}$ field. As the derivatives of the smoothed volume fraction can be determined by applying a convolution between the original volume fraction field and the derivatives of the kernel, the unit vector normal to the interface using the f field can be determined.

In both tests carried out in this work it was employed a sixth-order kernel ($\mathbf{K}_6$), like the one used by Francois *et al.* (2006).

2.3.3. Height function filtered by a convolution kernel (HF-fc)

This model is presented by Francois *et al.* (2006) as an interpolation scheme to estimate the curvature in the faces of the volume from its value in the center. In this work this model was employed to treat the anisotropy in the curvature field, which results from the HF method.

This model consists in applying a convolution operation to the curvature field obtained by the HF method, and therefore acts like a filter by considering the neighborhood in the average of the curvature in each volume:

$$\kappa_{i,j} = \frac{\sum_k \mathbf{K}\left(\mathbf{x'}_k - \mathbf{x}\right)\kappa\left(\mathbf{x'}_k\right)\Delta\mathbf{x'}_k}{\sum_k \mathbf{K}\left(\mathbf{x'}_k - \mathbf{x}\right)\Delta\mathbf{x'}_k}, \text{ for all } \mathbf{x'}_k \in \Omega_k \tag{11}$$

2.3.4. HF2 method

This last model is proposed by the authors as it was observed that the spurious currents generated by the HF method were associated to the local anisotropy of the curvature field and to errors in its estimation. The effects of these spurious currents are more pronounced in fine meshes.

As mentioned in the Section 2.3.1 the anisotropy in the curvature and the errors in its evaluation are generated by the scheme employed to estimate κ when the constrain imposed by Eq. (10) is not satisfied.

In the HF2 method an approach similar to that developed by Ferdowsi and Bussmann (2008) is used instead of the scheme applied in th HF method.

According to this approach the curvature in the volumes where Eq. (10) is not satisfied and where $0 < f_{ij} < 1$ is evaluated by a Taylor series centered at the nearest volume center, at which Eq. (10) is obeyed. This is the case illustrated by the volume $(i,j+1)$ in Fig. 1: in this volume $H_i < h_{j-1/2}$.

Thus in this new method the curvature in this volume can be approximated by

$$\kappa_{i,j+1} = \kappa_{i,j} + \left.\frac{d\kappa}{dx}\right|_{i,j} \Delta x_t \tag{12}$$

where the derivative is evaluated by differentiating Eq. (8) and by employing a 5x7-volumes stencil in order to estimate the third-order derivative of H, approximated by finite difference. The term Δx_t corresponds to the distance between the center of volume (i,j) and the middle-point of the interface at volume $(i,j+1)$, when it is approximated by a line (Fig. 2).
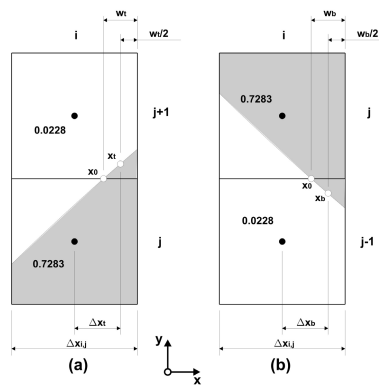
Figure 2. Examples of volumes at which the HF2 model can be applied.

The distances Δx_t and Δx_b illustrated in Fig. 2 are obtained by considering similarity of triangles and are equal to

$$\Delta x_t = \frac{1}{2(\beta+1)}\Delta x_{i,j} \quad and \quad \Delta x_b = \frac{\beta}{2(\beta+1)}\Delta x_{i,j} \tag{13}$$

where, for the cases shown in Fig. 2,

$$\beta = \begin{cases} \sqrt{\left|\dfrac{0,5[1-sign(n_y)]-f_{i,j+1}}{0,5[1+sign(n_y)]-f_{i,j}}\right|\dfrac{\Delta x_{i,j+1}\Delta y_{i,j+1}}{\Delta x_{i,j}\Delta y_{i,j}}}, & if\ 0 < f_{i,j+1}, f_{i,j} < 1 \\ \\ \sqrt{\left|\dfrac{0,5[1-sign(n_y)]-f_{i,j}}{0,5[1+sign(n_y)]-f_{i,j-1}}\right|\dfrac{\Delta x_{i,j}\Delta y_{i,j}}{\Delta x_{i,j-1}\Delta y_{i,j-1}}}, & if\ 0 < f_{i,j-1}, f_{i,j} < 1 \end{cases} \tag{14}$$

where n_y is the vertical component of the vector normal to the interface evaluate at the volume in which the curvature is desired.

The equations presented here correspond to the case in which the *y*-direction is dominant. Otherwise, the equations are analog.

The resulting curvature field obtained by the HF2 method is filtered by just taken a simply arithmetic average among the curvature of the volume and that of its neighbours which lie inside a circle with radius *R*.

3. TESTS AND RESULTS

In order to compare these curvature-models two two-dimensional test-cases were simulated: the static drop in equilibrium and the rising bubble in a resting fluid (Fig. 3).
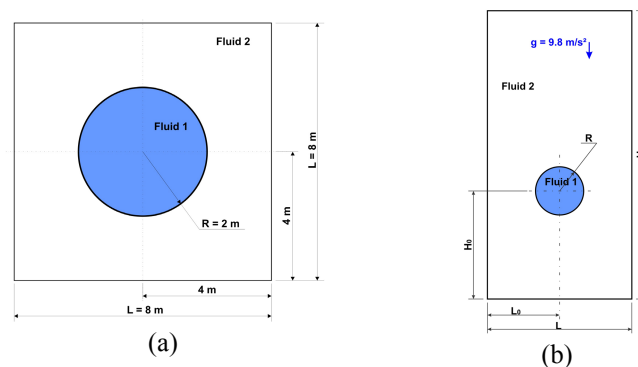

Figure 3. Test-cases: (a) Static drop and (b) Rising bubble.

Cartesian uniform meshes, as well as staggered arrangement of the variables, were employed in all the numerical simulations.

3.1. Static drop

In this case a two-dimensional static drop rests in the center of a square-domain immersed in another fluid. As the gravity is neglected, the interfacial tension effects are balanced by the gradient of pressure. Thus there should be no velocity field.

This test is divided into four cases. The values of the physical properties of both fluids and the parameters of the simulations for all these cases are shown in Tab. 1.

Table 1. Values of the parameters (static drop).

Case	Density Fluid 2 (kg/ m³)	Viscosity Fluid 1 (Pa s)	Viscosity Fluid 2 (Pa s)	Convergence criterium (u and v) (m/s)	Convergence criterium (p) (Pa)	Convergence criterium (f)
a. Inviscid 1	0.001	-	-			
b. Viscous 1	0.001	0.01	0.001	1E-14	1E-12	1E-12
c. Inviscid 2	0.1	-	-			
d. Viscous 2	0.1	0.01	0.001			

The following parameters were equal in all simulations: $\rho_l = 1$ kg/m^3, $\sigma = 73$ N/m (implying in an exact pressure jump equal to 36.5 Pa), and $\Delta t = 10^{-6}$ s. The simulations were carried out employing boundary condition of free-slip and impermeable walls in all boundaries and an initial field of $\mathbf{F}_{sv}$. The pressure as well as the components of velocity are null at t=0.

In order to estimate the order of the error in the main variables, five different mesh sizes where used: 20x20, 40x40, 80x80, 160x160 and 320x320 volumes.

3.1.1. Results of the static drop case

As previously mentioned in this test the velocity field should vanish. However, errors in evaluating the curvature of the interface result in the generation of spurious currents. In their paper, Francois and coworkers (2006) show that the generation of such currents is not limited to the CSF model, and conclude that the order of magnitude of these currents depends on the curvature-model employed.

Therefore the accuracy of the curvature-model can be measured in terms of the norm of the velocity field error: smaller this error, the more accurate is the evaluation of the curvature by the model. For this purpose the L_2 and L_∞ error norms will be employed. For the modulus of the velocity they are expressed as

$$L_2\left(\|\mathbf{u}\|\right) = \sqrt{\sum_{n=1}^{N}\|\mathbf{u}\|^2 \Big/ N} \tag{15}$$

$$L_\infty\left(\|\mathbf{u}\|\right) = max\left(\|\mathbf{u}\|\right) \tag{16}$$

where N is the total number of volumes.

In order to compare the results for the pressure field, the numerical jump in pressure is evaluated as (Francois *et al.*, 2006)

$$\Delta P_{total} = P_{in} - P_{out} \tag{17}$$

where the subscript "in" denotes inside the drop (averaged for volumes with $r \le R$) and "out" means outside the drop (averaged for volumes with $r > R$).

Francois and coworkers presented in their paper the error norms curves for the velocity and the jump in pressure only for the first case (Inviscid 1). These results are compared to those obtained in this work in Fig. 4.
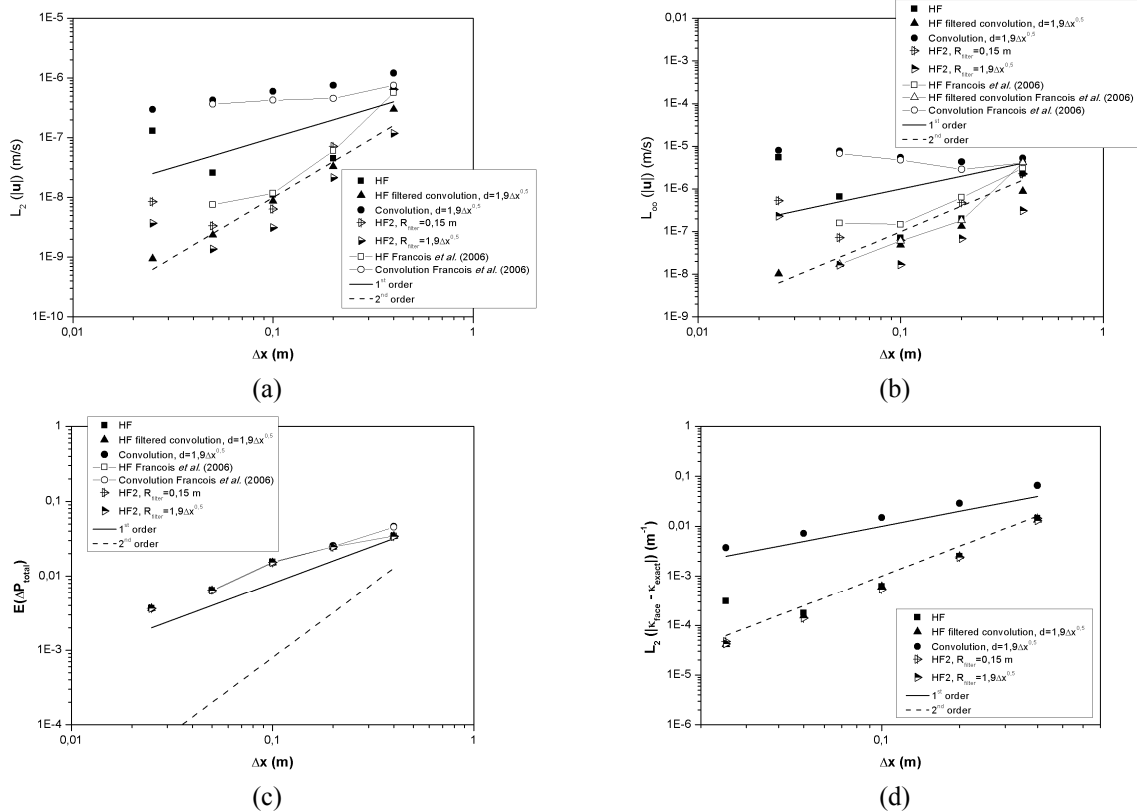
(a)

(b)

(c)

(d)

Figure 4. Error norms for the Inviscid 1 case: (a) L_2 norm of the velocity, (b) L_∞ norm of the velocity, (c) Error in the pressure jump and (d) L_2 norm of the curvature evaluated at the faces of the volumes.

The values of the kernel smoothing length and of the filter's radius employed in the simulations performed in this work are shown in the legends of Fig. 4. Francois *et al.* (2006) also set a kernel smoothing length equal to $1.9(\Delta x)^{0.5}$ in the convolution technique simulations – where Δx denotes the mesh resolution. But there is a lack of information in their paper concerning the value of this parameter used in the HF-fc model.

As can be seen in Fig. 4, although there is a good agreement between the results obtained in this work and those obtained by Francois and coworkers for the error in pressure jump, there are significant discrepancies between them in the L_2 and L_∞ error norms for the velocity. This difference is more expressive when the errors obtained by the HF method for the 160x160 volumes mesh (Δx=0.05 m) are compared in Fig. 4(a). While the errors for this method obtained in this work increase when meshes finer than 80x80 volumes are employed, in their paper the error obtained for a 160x160 volumes mesh maintain its decreasing tendency but not at the same rate of the remaining meshes.

When observing Fig. 4(b) it can be verified that this increasing tendency is also presented in the results obtained in this paper, as well as in those of Francois *et al*. This growth in the norm error is also verified in Fig. 4(d) for the L_2 norm of the curvature when employing a 320x320 volumes mesh, suggesting that there is a link between the error in evaluating the curvature of the interface and the generation of spurious currents. This association is supported when analyzing both the fields of the velocity norm and of the curvature errors: the regions with larger magnitudes of velocity correspond to those where the errors in the curvature are also larger. Besides this a local anisotropy can also be verified in the curvature errors field, which is due to the strategy adopted when the condition expressed in Eq. (10) is not satisfied.

The impact of such errors is softened when the approach implemented in the HF2 method is used in evaluating the curvature, while the effects of local anisotropy in curvature are expressively reduced when a kind of average – like the ones employed in the HF2 and in the HF-fc models – is applied to the curvature field, as can be seen in the results shown in Fig. 4 (a) and (b). This can also be concluded from the results of Francois and coworkers in Fig. 4(b).

Another important conclusion concerning the HF2 method is that as the filter's radius increases, the spurious currents decreases. However this model does not seem to be so efficient as the HF-fc method. Nevertheless these two models in addition to the HF method are better options to evaluate the curvature than the convolution technique, which results in first order errors for the three variables considered. These conclusions can also be drawn from the results of the other three cases of Tab. 1.

Comparing the errors obtained by each model for all the four cases it can be concluded that: the viscosity ratio between fluids 1 and 2 plays no role in the generation of spurious currents after one time step, and there is a slight difference among the results when the density ratio increases.

The spurious currents can also be measured by the total kinetic energy of the flow, as shown by Francois *et al.* (2006):

$$TKE = \frac{1}{2}\sum_{i=1}^{N}\rho_i V_i \mathbf{u}_i \cdot \mathbf{u}_i \qquad (18)$$

where i denotes the volume at which the kinetic energy is evaluated, and V represents its volume.

The estimation of *TKE* along time is an useful test of the capability of the curvature-models to damp the spurious currents, which is the desired behaviour.

After 500 time steps, as illustrated in Fig. 5, this behaviour is only reached by the HF method for the Inviscid 1 and Viscous 1 cases. These results were obtained by simulations employing a 40x40 volumes mesh and a Δt equal to 0.001 s.
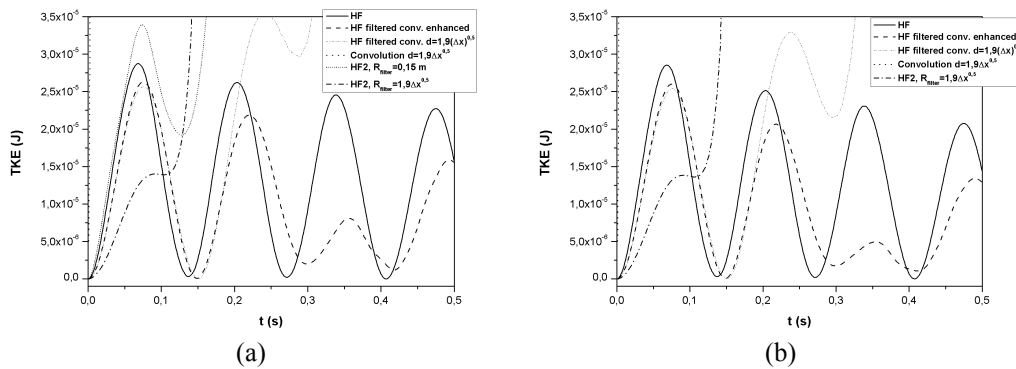

Figure 5. Temporal evolution of TKE for the (a) Inviscid 1 and (b) Viscous 1 cases after 500 time steps.

As time goes on the spurious currents are amplify when the Convolution technique (the almost vertical dotted line near the origin of both graphs), the HF-fc and the HF2 models are employed. Whereas the *TKE* obtained by the former two methods grows indefinitely, that provided by the HF2 method increases in a smaller rate until it stabilizes and reaches the equilibrium at *TKE* values of about 10^{-2} J.

This figure also shows the results obtained by the HF-fc enhanced model (dashed line). In this model the effects of the filter decrease exponentially with time, since its kernel smoothing length has the form

$$d = \left(1.9\sqrt{\Delta x}\right)exp\left(-2t\right) \qquad (19)$$

By softening the action of the filter along time, the spurious currents are damped, and therefore the total kinetic energy decreases in a smaller rate than that of the HF method. On the other hand, such a strategy was not able to produce the same behaviour when applied to the HF2 method and to the convolution technique.

Therefore the HF and the HF-fc enhanced methods are more able to deal with the unphysical velocity field effects than the other models when the temporal evolution is considered.

3.2. Rising bubble in a resting fluid

This test consists in simulating the flow of a bubble immersed in a tank filled with a heavier fluid. As the bubble raises toward the top of the domain, its shape changes. The rate of change depends on the magnitude of the interfacial tension coefficient: higher the value of this parameter, lesser the deformation of its surface.

Two cases were performed according the papers of Francois *et al.* (2006), Ginzburg and Wittum (2001) and Unverdi and Tryggvason (1992) and the values of the parameters employed in the numerical simulations are listed in Tab. 2 and 3.

Table 2. Values of the parameters of Francois case (rising bubble).

Parameter	Value
Density of Fluid 1 (kg/m³)	1.226
Density of Fluid 2 (kg/m³)	1000
Viscosity of Fluid 1 (Pa s)	1.137
Viscosity of Fluid 2 (Pa s)	1.78E-5
Interfacial tension (n/m)	728
Time step (s)	1E-5

Convergence criterium u and v (m/s)	1E-4
Convergence criterium p (Pa)	1
Convergence criterium f	1E-5
Mesh size	80x120 volumes

In the Francois case the following values of the dimensions indicated in Fig. 3b were employed: R=1/3 m, L=2 m, L_0=1 m, H=3 m and H_0=1 m. Therefore the Eötvös (Eo) number of the Francois case is equal to 5.98.

On the other hand, the values of these parameters used in the Ginzburg/Unverdi case are: R=1.67E-3 m, L=0.01 m, L_0=0.005 m, H=0.02 m and H_0 =0.75E-2 m. In both cases all the boundary conditions were set to free-slip and impermeable walls.

Table 3. Values of the parameters of Ginzburg/Unverdi case (rising bubble).

Case	Eötvös number	Morton number	μ_2/μ_1	Interfacial tension (N/m)	Time step (s)	Conv. crit. u and v (m/s)	Conv. crit. p (Pa)	Conv. crit. f	Mesh size
A	1	1E-4	493	0.109	1E-4	1E-6	1E-3	1E-5	32x64
B	10	1E-4	88	0.0109	5E-5	1E-5	1E-3	1E-5	64x128
C	104	1E-1	85	0.00105	5E-5	1E-5	1E-3	1E-5	256x512

In the Ginzburg/Unverdi case the values of the densities of fluid 1 and fluid 2 were set equal to 25 kg/m³ and 1000 kg/m³, respectively, while the dynamic viscosity of fluid 1 is equal to 1.22E-4 Pa s in all the simulations.

3.2.1. Results of the rising bubble case: Francois case

The numerical simulations of this case were carried out up to 0.5 s. And since the Eötvös number for this case is equal to 5.98, the interfacial tension plays an important role in defining the shape of the bubble.

Figure 6 illustrates the interface of the bubble obtained by each curvature-model at the end of simulations. The interface drawn in this figure was constructed by applying the PLIC technique.
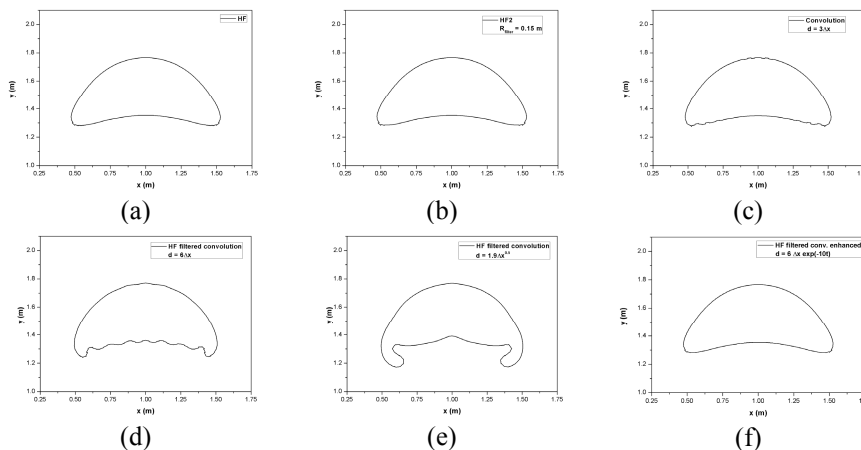

Figure 6. Bubble's interface obtained by (a) HF method, (b) HF2 method (R_{filter}=0.15 m), (c) Convolution technique (d=3Δx), (d) HF-fc (d=6Δx), (e) HF-fc (d=1.9$\Delta x^{0.5}$), and (f) HF-fc enhanced model (d= 6Δx exp[-10t]).

Whereas the interface obtained by the HF, HF2 and HF-fc enhanced models present no significant difference among each other and also when compared to that obtained by Francois and coworkers, the other two models exhibit expressive discrepancies in the shape of the interface.

The interface ondulations shown in Fig. 6 (c) and (d) seem to be a consequence of the spurious currents generated when the convolution technique and the HF-fc model are employed. This conclusion is corroborated by the result obtained by the HF-fc enhanced model, which presents no wavy interface since the filter acts only up to 0.18 s of simulation.

On the other hand the result produced by the HF-fc model in Fig. 6(e) suggests that the kernel smoothing length employed in the simulations was oversized, considering in the evaluation of curvature the contribution of volumes far away from the volume of interest.

3.2.2. Results of the rising bubble case: Ginzburg/Unverdi case

In this case the value of the Eötvös number varies from 1 to 104. The importance of interfacial tension effects decrease with increasing *Eo*.

For Eötvös equal to 1 (case A) the bubble's shape remains almost spherical after 600 time steps, while for *Eo* equal to 10 and 104 (cases B and C), the bubble's shape lie in the oblate ellipsoidal and spherical cap regimes, respectively. These last two simulations were carried out up to 1800 time steps.

Figure 7 shows the final shape of the bubble obtained in this work by employing the HF method for each of the cases listed in Tab. 3. For the cases A and B it is also illustrated the interface obtained by Ginzburg and Wittum (red dashed line). As can be observed there is excellent agreement between the results.
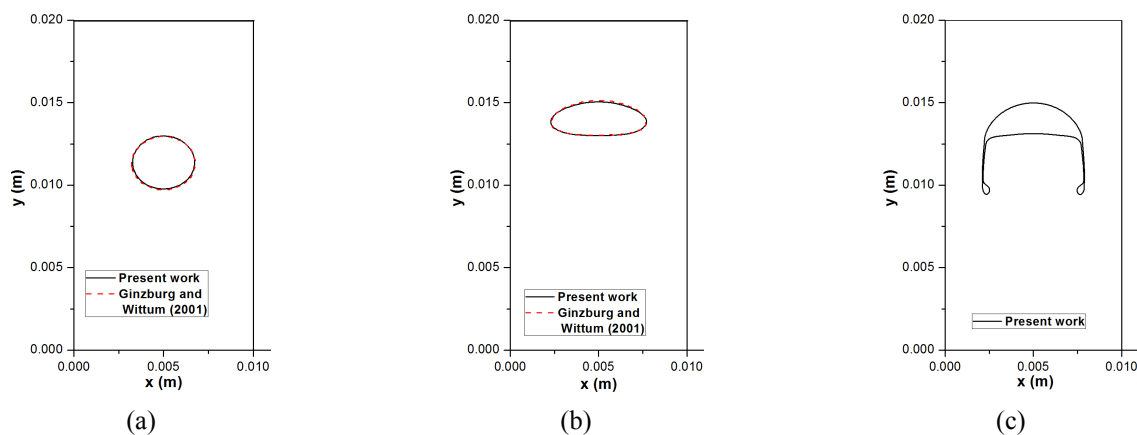

Figure 7. Rising bubble interface obtained in this work (continuous line) and by Ginzburg and Wittum (red dashed line): (a) case A, (b) case B, and (c) case C.

The bubble of case C developed a "skirt" after some time steps. This characteristic can also be observed in the results obtained by Ginzburg and Wittum (2001). Unfortunately such results could not be reproduced in this figure.

These results also agree qualitatively with those obtained by Unverdi and Tryggvason (1992).

As in the previous comparison, the results for the streamlines of the flow in a frame of reference moving with the bubble obtained in this work agree to those published by Ginzburg and Wittum, and by Unverdi and Tryggvason, suggesting that the HF method can deal satisfactory with the rising bubble problem, independently of the flow regime.

This problem was also simulated by employing the remaining curvature-models presented in this paper, in order to deem their performance. The results for the first two cases of Tab. 3 showed no expressive difference. However, when case C was carried out, the bubble obtained by the convolution technique exhibited a sequence of little bubbles in place of the skirt, while the results obtained by the other models show good agreement to those obtained by the HF method.

4. CONCLUSIONS

The performance of four curvature-models, including a model proposed by the authors (the HF2 method), was deemed in this work by numerically simulating two classic test-cases: the static drop in equilibrium and the rising bubble in a resting fluid.

In the static drop case when the L_2 error norm for the velocity was analyzed, the errors obtained by the convolution technique exhibited first-order convergence, while it was verified second-order convergence for the three other models. However, there is an increasing tendency in this error with increasing mesh resolution for the HF method results. This is also the overall behavior for the L_2 error norm of the curvature, suggesting that the errors in the curvature evaluation directly affect the generation of the spurious currents.

This increasing tendency is reduced when the curvature of the neighbour volumes is considered in the evaluation of the curvature of the volume of interest, that is, when some kind of filter is applied to the HF method. That is exactly the idea behind the HF2 and the HF-fc models. However it was proved that the application of such a filter should be constrained in time, otherwise the spurious currents will be amplified.

This conclusion can also be drawn from the results of the rising bubble tests, which show that good agreement to those published in literature is achieved by the HF and HF2 methods, while the effects of spurious currents are more pronounced in the results obtained by the other two models. It was also found that the results of the models involving convolution depend hardly on the chosen length of the kernel.

5. ACKNOWLEDGEMENTS

6. REFERENCES

Brackbill, J., Kothe, D. and Zemach, C., 1992, "A continuum method for modeling surface tension", Journal of Computational Physics, Vol. 100, No. 2, pp. 335-354.

Ferdowsi, P. and Bussmann, M., 2008, "Second-order accurate normals from height functions", Journal of Computational Physics, Vol. 227, No. 22, pp. 9293-9302.

Francois, M., Cummins, S., Dendy, E., Kothe, D., Sicilian, J. and Williams, M., 2006, "A balanced-force algorithm for continuous and sharp interfacial surface tension models within a volume tracking framework", Journal of Computational Physics, Vol. 213, No. 1, pp.141-173.

Ginzburg, I. and Wittum, G., 2001, "Two-phase flows on interface refined grids modeled with VOF, staggered finite volumes, and spline interpolants", Journal of Computational Physics, Vol. 166, No. 2, pp.302-335.

Hirt, C.W. and Nichols, B.D., 1981, "Volume of Fluid (VOF) Method for the Dynamics of Free Boundaries", Journal of Computational Physics, Vol. 39, No. 1, pp. 201-225.

Kothe, D.B., Rider, W.J., Mosso, S.J., Brock, J.S. and Hochstein, J.I., 1996, "Volume Tracking of Interfaces Having Surface Tension in Two and Three Dimensions", Aerospace Sciences Meeting and Exhibit, 34th, Reno: AIAA 96-0859.

López, J., Zanzi, C., Gómez, P., Zamora, R., Faura, F. and Hernández, J., 2009, "An improved height function technique for computing interface curvature from volume fractions", Computer Methods in Applied Mechanics and Engineering, Vol. 198, No. 33-36, pp. 2555-2564.

Malik, M. and Bussmann, M., 2004, "Volume Tracking on Adaptively Refined Grids with Curvature Based Refiement", Proceedins of CSME Forum, London, UK, pp. 1-10.

Malik, M., Fan, E. and Bussmann, M., 2007, "Adaptive VOF with curvature-based refinement", International Journal for Numerical Methods in Fluids, Vol. 55, No. 7, pp. 693-712.

Maliska, C.R., 2004, "Transferência de calor e mecânica dos fluidos computacional", LTC – Livros Técnicos e Científicos Editora S. A., Rio de Janeiro, Brazil, 453 p.

Sussman, M. and Ohta, M., 2006, "High-order techniques for calculating surface tension forces", In: International Series of Numerical Mathematics, Basel, Switzerland, Vol. 154, pp. 425-434.

Unverdi, S. and Tryggvason, G., 1992, "A front-tracking method for viscous, incompressible, multi-fluid flows", Journal of Computational Physics, Vol. 100, No. 1, pp. 25-37.

Williams, M., Kothe, D. and Puckett, E., 1998, "Accuracy and convergence of kernel-based continuum surface tension models", Technical Report LA-UR-98-2268, Los Alamos National Laboratory, USA, 15 p.

7. RESPONSIBILITY NOTICE

The authors are the only responsible for the printed material included in this paper.